Orientation and length scale effects on dislocation structure in highly oriented nanotwinned Cu

Lu, Qiuhong; Huang, Xiaoxu; Hansen, Niels; Lu, Lei

Published in:
I O P Conference Series: Materials Science and Engineering

Link to article, DOI:
10.1088/1757-899X/219/1/012032

Publication date:
2017

Document Version
Publisher's PDF, also known as Version of record

Orientation and length scale effects on dislocation structure in highly oriented nanotwinned Cu

To cite this article: Qiuhong Lu *et al* 2017 *IOP Conf. Ser.: Mater. Sci. Eng.* **219** 012032

IOP Conf. Series: Materials Science and Engineering **219** (2017) 012032 doi:10.1088/1757-899X/219/1/012032

Orientation and length scale effects on dislocation structure in highly oriented nanotwinned Cu

Qiuhong Lu[1], Xiaoxu Huang[2], Niels Hansen[2], Lei Lu[1*]

[1] Shenyang National Laboratory for Materials Science, Institute of Metal Research, Chinese Academy of Sciences, Shenyang, 110016, PR China
[2]Section for Materials Science and Advanced Characterization, Department of Wind Energy, Technical University of Denmark, Risø Campus, DK-4000, Roskilde, Denmark

*Email: llu@imr.ac.cn

Abstract. Highly oriented nanotwinned Cu has been compressed to 6% strain in directions 90°, 0° and 45° with respect to the twin boundaries of the almost parallel twins. In the 90° and 0° compressed samples Mode I and Mode II dislocations and their interactions with twin boundaries dominate the deformation of twin/matrix (T/M) lamellae with thickness less than 500 nm. In 45° compressed samples, Mode III dislocations, especially partial dislocations moving along the twin boundaries, dominate the deformation of fine T/M lamellae with thickness less than 100 nm, while dislocations from slip Modes I, II and III are identified in T/M lamellae more than 100 nm thick, where these dislocations extensively interact in the T/M lamellae with thicknesses more than 200 nm. Dislocation cells are observed in a twin lamella with a thickness of about 500 nm.

1. Introduction

Plastic deformation of metallic materials involves glide, interactions, and storage of dislocations. Important parameters are the structural characteristics and the loading conditions determining the number of potential slip systems, and which of these active [1]. For fcc and bcc single crystals and poly-crystals deforming by multi-slip, the structural evolution follows a universal pattern of structural subdivision by the formation of cell blocks and cells [2]. For small strains, the size of these features are in the micrometer/submicrometer range and their characteristics depend on the crystallographic orientation of the material in which they form and evolve [2, 3]. However, the structural scale is also important as there appears to be a limit of about 5 μm below which a well-defined cell block structure does not form. Examples are deformed and recrystallized Cu with a grain size of about 4 μm [4] and spark plasma sintered Al with a grain size of about 5 μm [5]. This limit may, however, be lower as cell blocks have been observed in twin/matrix (T/M) lamellae with a thickness of 0.5-1 μm in rolled nano-twinned (nt) Cu [6] processed by electrodeposition. The effects of orientation and structural scale on the evolution of deformation microstructure have therefore been chosen as the topic of the present research. The material is electrodeposited nt-Cu with T/M lamellar thickness ranging from tens to hundreds of nanometers [6] which has been compressed in three directions: 90°, 0° and 45° with respect to the twin plane. Samples have been compressed up to a strain of 6% where different slip modes and combinations of slip modes will be activated [7-13]. The deformed microstructure has been analyzed by TEM focusing on individual dislocations, dislocation-dislocation interactions and

dislocation-twin boundary (TB) interactions. The T/M lamellar thickness covers different length scales, namely <100 nm, 100-200 nm and <500 nm.

2. Experimental

High-purity Cu sheets with nanoscale growth twins were synthesized by means of direct-current electro-deposition from an electrolyte of $CuSO_4$. More details about the deposition parameters are described in Ref. [7]. The nt-Cu sheet was deposited to a final thickness of more than 1.5 mm by carefully controlling the deposition parameters. The microstructure the as-deposited Cu specimens has been observed and is shown in figure 3 in Ref. [7]. The as-deposited Cu sample consists of micron/submicron-sized columnar grains with {111} out-of-plane texture. The grain size exhibits a distribution from 1 to 6 μm (with an average value of about 3 μm). These columnar grains are subdivided by nanoscale twin lamellae, most of which are parallel to the deposited sheet plane. Statistical analysis indicates that the twin thickness is about 30 nm on average, and varies from a few nanometers to about 500 nm.

Compression samples were cut from the as-deposited Cu sheets and then mechanically polished to a rectangular cuboid of $0.8 \times 0.8 \times 1.2$ mm^3. Uniaxial compression tests at room temperature were performed on an Instron 5848 microtester with a 2 kN load cell at a strain rate of 1×10^{-3} s^{-1}. The compression direction is parallel to the TBs (0° compression), perpendicular to the TBs, and at 45° with respect to the TBs (45° compression). The cross-head displacement was used to determine the imposed strain, with corrections for machine compliance. In this study, the total compression strain is ~6%.

Microstructures of specimens before and after compression were characterized using a FEI Tecnai F20 transmission electron microscope at an accelerating voltage of 200 kV. To examine the dislocation configurations and contributing Burgers vectors $\boldsymbol{b}$ of dislocation structures, two-beam diffraction contrast experiments were carried out in the TEM employing different diffraction vectors, $\boldsymbol{g}$, using the $\boldsymbol{g}\cdot\boldsymbol{b} = 0$ invisibility criterion [14].

Slip systems in nt-Cu can be divided into three categories according to their geometrical relations to the twin boundary plane: Mode I, where both slip plane and slip direction of the active slip systems are inclined to the TB, Mode II, where the slip plane is inclined to TB but the slip direction parallel to the TB, and Mode III, where both the slip plane and slip direction are parallel to the TB. According to the two beam TEM analysis, dislocations from different slip modes can be distinguished based on their visibility under different two beam conditions. With $\boldsymbol{g_M}=\boldsymbol{g_T}=111$, Mode I dislocations with Burgers vectors $\boldsymbol{b1}=1/2[011]$, $\boldsymbol{b2}=1/2[110]$, $\boldsymbol{b3}=1/2[101]$ are all visible, while the Mode II or Mode III dislocations $\boldsymbol{b4}=1/2[1\bar{0}1]$, $\boldsymbol{b5}=1/2[01\bar{1}]$, $\boldsymbol{b6}=1/2[1\bar{1}0]$ are all invisible, enabling separation of Mode I dislocations from Mode II and Mode III dislocations. Dislocations from Mode III and II slip systems have the same Burgers vectors ***b4, b5*** and ***b6***, but the dislocation lines of Mode III dislocations must be parallel to the TBs.

3. Results

Figure 1a shows typical observations of dislocation structures from the 90° compressed nt-Cu sample, which was taken with a $\boldsymbol{g}$ vector of $\boldsymbol{g_M}=\boldsymbol{g_T}=[111]$. These dislocations are all visible under $\boldsymbol{g_M}=\boldsymbol{g_T}=[111]$, indicating that they have Burgers vectors of ***b1, b2*** or ***b3*** and belong to Mode I slip systems according to above analysis. Most dislocations are accumulated at the TBs and only a few dislocation segments (red arrows in figure 1a) are retained within the matrix and twin lamellae. The dislocation densities are not related very much to the thickness scale of the T/M lamellae. But when the T/M lamellae are very thin, the density of TBs is high, and presents a morphology with very high dislocation density in the fine twin lamellae ("F" in figure 1a). It should be noted that few dislocation interactions or tangling are seen inside the twin lamellae even in the twin lamellae with a thickness of about 200 nm ("C" in figure 1a).

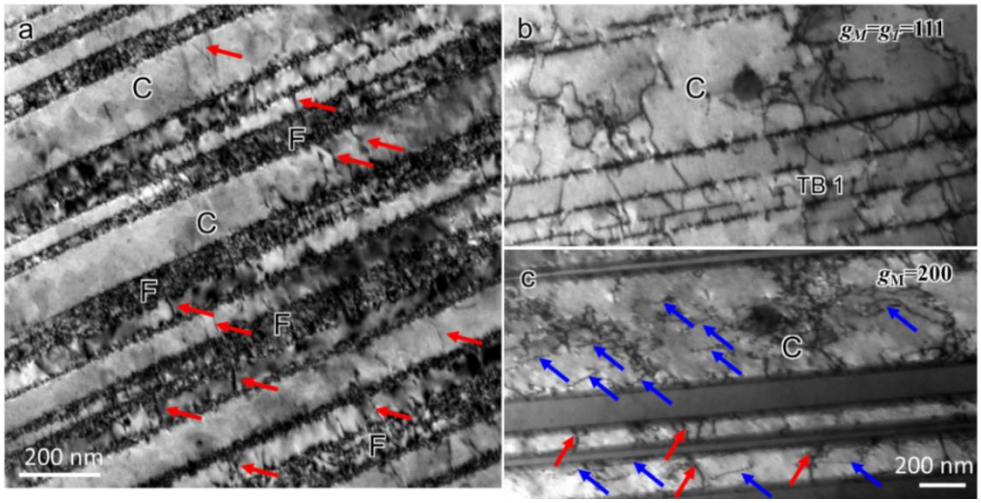

Figure 1. Two-beam diffraction images of dislocations under $\boldsymbol{g_M}=\boldsymbol{g_T}=[111]$ in 90º compression (a) and under $\boldsymbol{g_M}=\boldsymbol{g_T}=[111]$ (b) and $\boldsymbol{g_M}=[002]$ (c) in 0º compression of nt-Cu. The red and blue arrows point out the Mode I and II dislocations, respectively. The fine lamellae with a thickness less than 100 nm are marked "F"; the coarse lamellae with a thickness more than 100 nm are marked "C".

Figures 1b and 1c are typical two-beam diffraction TEM images of the nt-Cu under 0° compression analyzed under $\boldsymbol{g_M}=\boldsymbol{g_T}=[111]$ and $\boldsymbol{g_M}=[200]$, respectively. Observing using $\boldsymbol{g_M}=\boldsymbol{g_T}=[111]$ (figure 1b), Mode I dislocations are clearly seen both in the twin lamellae and on the TBs. The dislocations accumulated on the TBs between fine T/M lamella ("TB 1" in figure 1b) are much less numerous than those between the fine T/M lamellae in 90º compression ("F"s in figure 1a). Observing from $\boldsymbol{g_M}=[200]$ (figure 1c), many short dislocation lines slightly inclined to the TBs (blue arrows in figure 1c) are seen. These dislocations are all invisible under $\boldsymbol{g_M}=\boldsymbol{g_T}=[111]$, indicating that they have Burgers vectors of $\boldsymbol{b4}$ or $\boldsymbol{b6}$ and belong to Mode II slip systems. For the twin lamellae with a thickness of less than 200 nm, Mode II dislocations inside the twin lamellae appear to be as numerous as Mode I dislocations. Higher magnification observations in our former investigations [5] indicate, however, that the density of Mode II dislocations is much higher than that of Mode I dislocations but can only be identified by the tails on the TBs. In the twin lamellae with a thickness of more than 500 nm ("C" in figure 1b and 1c), a high density of Mode II dislocations and a few Mode I dislocations are sene and a small extent of dislocation interactions between Mode I and Mode II dislocations is observed. The TEM observations in figure 1 indicate that Mode I and Mode II dislocations dominate the deformation of T/M lamellae with thickness less than 500 nm in 90° and 0° compressions, respectively. Few dislocation interactions happen in twin lamellae less than 500 nm thick when compressed in either the 90º or 0º directions.

Figures 2a and 2b present the typical dislocation structures of T/M lamellae with a thickness less than 200 nm thick in the 45º compressed nt-Cu sample under $\boldsymbol{g_M}=[200]$. Few dislocations appear inside the fine T/M lamellae less than 100 nm thick ("F" in figure 2). As for the twin lamellae of 100-200 nm thick ("C1" in figure 2), different from the observations in 90° and 0° compressed samples, more dislocations inside the T/M lamellae and some dislocation interactions are observed. The dislocations types can be simply distinguished by their morphologies. Dislocation lines cutting through the TBs are Mode I dislocations (red arrows in figure 2a). Mode II dislocations (blue arrows in figure 2a) have dislocation lines slightly inclined to the TBs. However no Mode III dislocations are found inside the T/M lamellae. It is interesting to see that there are plenty of dislocations appearing on the TBs of all the T/M lamellae in shown in figure 2. Additional analysis has shown that these dislocations are all invisible under $\boldsymbol{g_M}=\boldsymbol{g_T}=[111]$, indicating that these are Mode III dislocations with Burgers vectors of $\boldsymbol{b4}$ or $\boldsymbol{b6}$ slipping on the TBs. Careful observations show that the dislocations on the

TBs present two different morphologies. A few dislocations have sharp and clear dislocation lines (arrows "1" in figure 2b), but most dislocations observed show a morphology of wide dark layers (arrows "2" in figure 2b), which should be the twinning partial dislocations. Twinning partials on the TBs have Burgers vectors of δA or δB or δC, can be classified as Mode III dislocations, and may also be visible under $\boldsymbol{g}_M$ = [200] ($\boldsymbol{g}\cdot\boldsymbol{b}$=1/3, 2/3 and 1/3, respectively). It is obvious that dislocations from Mode III slip systems, especially partial dislocations slipping on the TBs, dominate the deformation of twin lamellae less than 200 nm thick in 45° compression. These observations are consistent with the previous investigations [7].

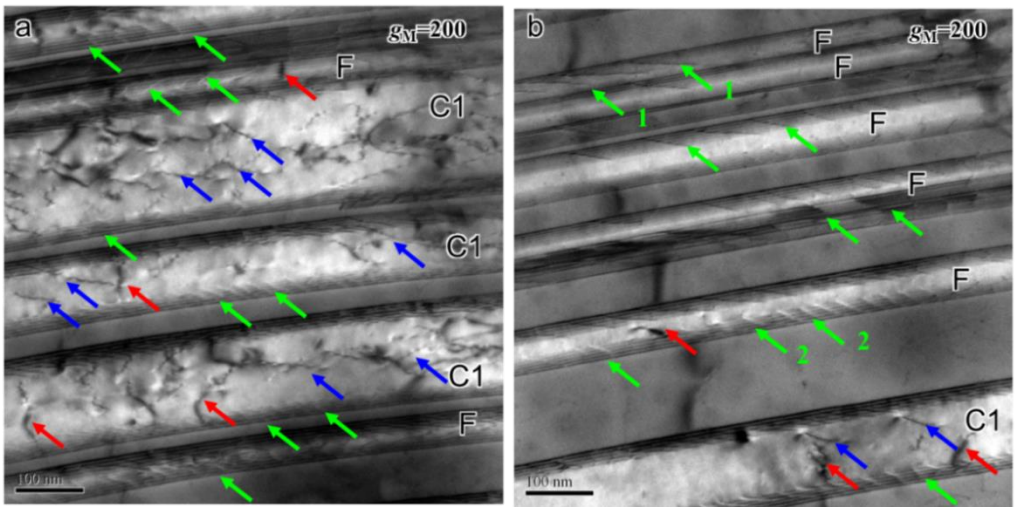

Figure 2. Enlarged two-beam diffraction images showing dislocations in coarse (a) and fine (b) twin lamellae of 45º compressed nt-Cu under under $\boldsymbol{g}_M$=200. The red, blue and green arrows point out the Mode I, II and III (Shockley partial) dislocations, respectively. Arrows "1" marked out two perfect Mode III dislocations on the TB. Arrows "2" marked out two partial Mode III dislocations on the TB. The fine lamellae with a thickness less than 100 nm are marked "F"; the coarse lamellae with a thickness of 100-200 nm are marked "C1".

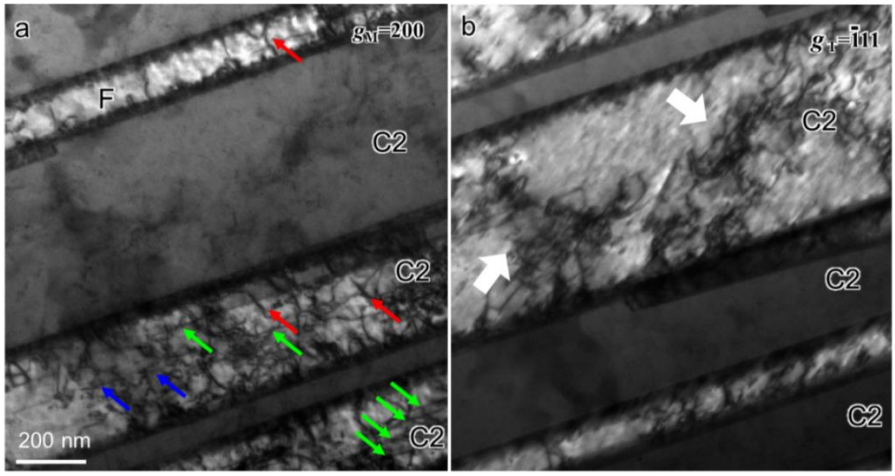

Figure 3. Two-beam diffraction images of dislocations in coarse twin lamellae of 45º compressed nt-Cu under $\boldsymbol{g}_M$=002 (a) and $\boldsymbol{g}_M$ = $\bar{1}11$ (b). The red, blue and green arrows point out the Mode I, II and III dislocations, respectively. Dislocations from slip Modes I, II and III interacting in the twin lamella "C2"; and dislocation cells formed in twin lamella "C2" (about 500 nm) pointed out by white arrows.

Figures 3a and 3b show the typical dislocation structures of coarse T/M lamellae with a thickness of more than 200 nm ("C2" in figure 2) in the nt-Cu sample under $\boldsymbol{g_M}$ = [200] and $\boldsymbol{g_T}$ =[$\bar{1}$11] compressed in 45° direction with respected to the TBs. Compared with the coarse lamellae of 100- 200 nm thick ("C1" in figure 2), more Mode I (red arrows) and Mode II (blue arrows) dislocations appear inside these lamellae. Furthermore, Mode III dislocations (green arrows in figure 3a) with dislocation lines parallel to the TBs are observed inside the lamellae. Most dislocations are tangled inside the T/M lamellae. In a twin lamella with a thickness of about 500 nm dislocations are seen to tangle extensively and appear to be evolving into dislocation cell structures (white arrows in figure 3b).

4. Discussion

When analyzing the dislocation structure one must take into account that the samples have been cold-compressed to the strain of 6%. The microstructure therefore represents a work hardened state. In a previous study [7], samples have been analyzed after 2% and 6% compression, where a significant effect of strain on the microstructure has been found. An example is that slip transmission across twin boundaries is observed after 2% compression both in the 90° and in the 0° compressed samples, most pronounced in the former. By raising the strain to 6%, the frequency of slip transmission is reduced.

Based on such observations and taking the Schmid factor into account (Table 1) the microstructure will be analyzed in the following, separately for the three loading directions.

Table 1. Active slip systems and corresponding Schmid factors for the 90°, 0° and 45° compression.

Loading direction	90°	0°	45°
Active slip systems	Mode I dominant	Mode I and II; (Mode II dominant)	Mode I, II and III (Mode III dominant)
Maximum Schmid factors [7]	Mode I: 0.272; Mode II, III: 0	Mode I: 0.408; Mode II: 0.470; Mode III: 0	Mode I: 0.484; Mode II: 0.360; Mode III: 0.5

In 90° compressed samples, slip Mode I dominates with 6 active slip systems. In 0°compressed samples, slip Modes I and II are active, involving totally 9 systems. In 45°compressed samples, Modes I, II and III are active with 12 systems. As there are 12 systems in the twin and 12 in the matrix, the total number of systems is 21 as 3 systems in the slip plane are common to the twin and the matrix.

To analyze the microstructural characteristics in relation to the active slip systems, the slip distance, which is the distance from a dislocation source to a dislocation barrier (in the present case, a twin boundary), must also be taken into account. Dislocation sources can be grain boundaries, with a spacing of about 3 μm, and twin boundaries, with an average spacing of 30 nm. In general, it is expected that the flow stress decreases with increasing slip distance, which has been verified previously in [8] where the yield stress decreases with an expected increasing in slip distance when the loading direction is changed from 90° to 0° and from 0° to 45°. It follows that in the 90° compressed samples, the slip distance is small, of the order of the twin thickness. Dislocation-dislocation interaction is negligible and at 6% strain, the majority of dislocations are stored at or near the twin boundaries. Therefore a small effect of the structural scale is expected as is observed. In 0° compressed samples, the slip modes are I and II and the slip distance is only slightly larger than that in 90°, and therefore there is not a significant effect on the structural scale. Dislocations are stored at or near the twin boundaries and dislocation-dislocation interaction is only occasionally observed at the larger length scale of 200-300 nm. In 45° compression, with 3 active slip modes and a large slip distance, the effect of the structural scale is significant. With T/M lamellar thickness in the range 200-500 nm dislocation-dislocation interactions are frequent and dislocations can move in 3 dimensions as shown by the presence of dislocation cells (see Fig 3). However, when the structural scale is reduced to 50-200 nm, mode III will dominate with dislocations moving at, and parallel with, the twin boundaries, and the resulting structure in the T/M lamellae contains only isolated dislocations.

In the present analysis, the relationship between active slip systems and the deformation microstructure shows a strong effect of loading direction. A similar effect on the flow stress and work hardening behavior is also expected, which has been observed [8] and is to be further analyzed in a forthcoming paper.

5. Conclusions

Highly oriented nt-Cu, with the T/M lamellar thickness varying from a few nanometers to about 500 nm and being 30 nm on average, has been compressed to 6% strain in directions of 90°, 0° and 45° with respect to the TBs of the almost parallel twins. The dislocation structures in T/M lamellae with different thicknesses have been characterized. It is found that the active slip systems and dislocation configurations are strongly dependent on the loading direction.

In the 90° and 0° compressed samples, mode I and mode I + mode II, respectively, dominate the deformation of T/M lamellae with thicknesses in the range of 50-500 nm. Some dislocations are observed in the T/M lamellae but most dislocations are accumulated at the twin boundaries.

In the 45° compressed sample, a clear length scale effect is observed. In the range 200-500 nm, all three slip modes (I, II, and III) are active, and dislocation interactions can take place in the T/M lamellae resulting in the formation of dislocations cells. In the range of 50-200 nm, slip mode III dominates with dislocations moving at, and parallel to, the twin boundaries, with some isolated dislocations stored in the T/M lamellae.

Acknowledgements

This research was supported by National Nature Science Foundation of China (Nos. 51420105001, 51371171, 51101163, 51401211 and U1530146).

References

[1] Kocks UF, Canova GR 1981, in *Proc. of 2nd Risø Inter. Sym. on Mater. Sci. (Roskilde)*, 35–44
[2] Hansen N, Huang X, Pantleon W, Winther G 2006 *Philos. Mag*. **86** 3981–94
[3] Huang X, Winther G 2007 *Philos. Mag.* **87** 5189–214
[4] Huang X, Hansen N 2004 *Mater. Sci. Eng.* **387–389** 186–90
[5] Le GM, Godfrey A, Hansen N, Liu W, Winther G, Huang X 2013 *Acta Mater.* **61** 7072–86
[6] Lu QH, Sui ML, Huang X, Li DX Hansen N 2014 *Philos. Mag.* 94 2262–80
[7] Lu QH, You ZS, Huang X, Hansen N, Lu L 2017 *Acta Mater.* **127** 85–97
[8] You ZS, Li XY, Gui LJ, Lu QH, Zhu T, Gao HJ, Lu L 2013 *Acta Mater.* **61** 217–27
[9] Li XY, Wei YJ, Lu L, Lu K, Gao HJ 2010 *Nature* **464** 877–80
[10] Zhang X, Misra A 2004 *J. Appl. Phys.* **96** 7173–8
[11] Wang J, Li N, Misra A 2013 *Philos. Mag.* **93** 315–27
[12] Hodge AM, Wang YM, Barbee TW, Jr. 2008 *Scr. Mater.* **59** 163–6
[13] Deng C, Sansoz F 2009 *Nano Letters* **9** 1517–22
[14] Williams D, Carter CB, 2009 *Transmission Electron Microscopy*, Springer US, 3–22